

# Boundary-Aware Vision Transformer for Angiography Vascular Network Segmentation

Nabil Hezil<sup>1,2</sup>, Suraj Singh<sup>4</sup>, Vita Vlasova<sup>3,5</sup>, Oleg Rogov<sup>3,4,6</sup>, Ahmed Bouridane<sup>1,7</sup>, Rifat Hamoudi<sup>7</sup>

<sup>1</sup>College of Computing and Informatics, University of Sharjah, UAE

<sup>2</sup>Scientific and Technical Research Center for the Development of Arabic Language (CRSTDLA), Algeria

<sup>3</sup>Artificial Intelligence Research Institute, Moscow, Russia

<sup>4</sup>Skolkovo Institute of Science and Technology, Moscow, Russia

<sup>5</sup>Bauman Moscow State Technical University, Moscow, Russia

<sup>6</sup>Moscow Technical University of Communications and Informatics, Moscow, Russia

<sup>7</sup>BIMAI-Lab, Biomedically Informed Artificial Intelligence Laboratory, University of Sharjah, UAE

Corresponding author email: rogov@airi.net

**Abstract**—Accurate segmentation of vascular structures in coronary angiography remains a core challenge in medical image analysis due to the complexity of elongated, thin, and low-contrast vessels. Classical convolutional neural networks (CNNs) often fail to preserve topological continuity, while recent Vision Transformer (ViT)-based models, although strong in global context modeling, lack precise boundary awareness. In this work, we introduce BAVT, a Boundary-Aware Vision Transformer, a ViT-based architecture enhanced with an edge-aware loss that explicitly guides the segmentation toward fine-grained vascular boundaries. Unlike hybrid transformer-CNN models, BAVT retains a minimal, scalable structure that is fully compatible with large-scale vision foundation model (VFM) pretraining. We validate our approach on the DCA-1 coronary angiography dataset, where BAVT achieves superior performance across medical image segmentation metrics outperforming both CNN and hybrid baselines. These results demonstrate the effectiveness of combining plain ViT encoders with boundary-aware supervision for clinical-grade vascular segmentation.

**Index Terms**—Vision Transformer, Vascular Segmentation, Coronary Angiography Medical Image Analysis, Deep Learning.

## I. INTRODUCTION

Interpreting angiography X-rays and CT coronary images is a complex and time-consuming task that requires significant clinical expertise [1], [2]. These imaging modalities are essential for diagnosing vascular diseases, including coronary artery disease, yet their analysis presents unique challenges due to intricate vessel structures, varying contrast levels, and subtle pathological features [3]. Errors in interpretation can lead to misdiagnoses and delayed treatments, underscoring the need for reliable automated solutions. The growing volume of angiographic studies, particularly in high-demand clinical settings, exacerbates diagnostic delays, further motivating the development of robust computational tools [4], [5].

Automated vascular analysis can be approached as a segmentation and feature extraction task. While recent advances in deep learning, such as encoder-decoder architectures [1], [2] and transformer-based models [6], have shown promise, accurately segmenting fine vessel structures—especially in low-contrast regions—remains an unresolved challenge. Key

difficulties include distinguishing small vessels from noise, handling varying imaging conditions, and preserving topological correctness in segmented vascular networks.

This work focuses on developing an enhanced transformer-based approach for vascular segmentation in angiography and CT coronary imaging. We adapt a state-of-the-art encoder-decoder architecture [7] by incorporating multi-scale feature fusion, attention mechanisms, and curriculum learning to improve small-vessel detection. Our method is evaluated on the DCA-1 dataset, achieving an F1 score of 0.81, demonstrating superior performance in capturing fine vascular details. Unlike existing approaches [8], [9], our enhancements do not increase computational complexity during inference, making the method suitable for clinical deployment.

A critical challenge in vascular image analysis is the accurate segmentation of peripheral and microvascular structures [10]. We demonstrate that curriculum learning significantly improves performance in this aspect—a factor overlooked in prior work. Given the clinical importance of detecting early-stage vascular abnormalities, we argue that this direction warrants further research within the medical imaging community.

## II. RELATED WORK

### A. Vision Transformers for Medical Image Segmentation

Transformers, originally introduced for natural language processing [11], have shown strong potential in vision tasks through the Vision Transformer (ViT) [12]. ViT segments images into fixed-size patches, processes them globally via self-attention, and has shown competitive performance when pre-trained on large-scale datasets. For segmentation, this global context modeling can be beneficial, but ViTs lack inherent inductive biases for locality and scale, which are often critical in medical imaging, especially for thin or branching structures such as vessels.

To address these limitations, various adaptations have been proposed. Swin Transformer [13] and SegFormer [14] introduce hierarchical attention and multi-scale fusion, while ViT-Adapter [15] incorporates convolutional modules to restore spatial priors. However, these models depart from the plain

ViT architecture, which hinders compatibility with modern vision foundation model (VFM) pretraining pipelines such as DINOv2 [16] or EVA-02 [17], both of which favor vanilla ViT backbones for scalability.

Recent efforts like UViT [18] and YOLOS [19] retain the plain ViT structure, yet are primarily designed for classification or detection. In contrast, our work leverages fully pre-trained ViTs with minimal decoder overhead, enhanced by a boundary-aware loss to explicitly guide fine-grained vascular segmentation.

### B. Vessel Segmentation and Transformer-Based Architectures

Accurate vessel segmentation remains a key challenge due to the thin, branching, and low-contrast nature of vascular structures. Earlier CNN-based approaches such as U-Net [20] have been widely adopted but struggle to maintain detail at the microvascular level.

To mitigate this, recent transformer-based hybrid models have been proposed. HT-Net [21] introduced transformer blocks into a U-Net-style backbone to capture global dependencies and incorporated dedicated refinement modules for vessels of varying sizes. Similarly, MTPA-UNet [22] fused convolutional encoders with self-attention modules to improve multi-scale representation learning, demonstrating improved segmentation accuracy on vascular datasets.

These hybrid methods validate the utility of attention mechanisms in vascular modeling. However, they still rely on custom modules, complex decoders, or architectural specializations. In contrast, our Boundary-Aware Vision Transformer (BAVT) introduces an edge-aware loss into a lightweight, ViT-based pipeline that remains compatible with scalable VFM pretraining and exhibits strong performance with minimal architectural tuning.

### C. Pretraining and Generalization in Medical Vision

Large-scale pretraining has become a cornerstone of high-performing vision models. While early efforts used supervised classification on ImageNet [23], recent advances in self-supervised masked modeling [16], [17], [24] have led to powerful foundation models for vision tasks. These models, particularly DINOv2 and EVA-02, leverage ViT backbones and offer excellent feature quality for downstream segmentation [25], [26].

Non-ViT architectures such as Swin [13] and ConVNeXt [27] cannot directly benefit from such pretraining due to architectural incompatibility. Our proposed model is fully ViT-compatible and can leverage these foundation models for enhanced generalization on challenging medical datasets such as DCA-1, where vascular features are subtle and spatial resolution is limited.

## III. METHOD

### A. Problem Statement

Let  $\mathbf{X} \in \mathbb{R}^{H \times W}$  denote a grayscale angiographic image, where  $H = W = 512$ , and let  $\mathbf{Y} \in \{0, 1\}^{H \times W}$  be the corresponding binary ground truth mask, where 1 indicates

vessel pixels. Our goal is to learn a segmentation function  $f_\theta : \mathbb{R}^{H \times W} \rightarrow [0, 1]^{H \times W}$  parameterized by  $\theta$ , which produces a soft segmentation map  $\hat{\mathbf{Y}} = f_\theta(\mathbf{X})$  that closely matches  $\mathbf{Y}$  in both region and boundary accuracy.

Let us now divide the input image  $\mathbf{X}$  into  $N_p = (H \times W)P^{-2}$  non-overlapping square patches of size  $P \times P$  (e.g.,  $P = 16$ ), such that each patch  $\mathbf{x}_i \in \mathbb{R}^{P \times P}$ . These are flattened and linearly projected into a  $D$ -dimensional token space:

$$\mathbf{z}_i^{(0)} = \mathbf{E} \cdot \text{vec}(\mathbf{x}_i) + \mathbf{p}_i, \quad i = 1, \dots, N_p, \quad (1)$$

where  $\mathbf{E} \in \mathbb{R}^{D \times P^2}$  is a learnable projection matrix and  $\mathbf{p}_i \in \mathbb{R}^D$  is a positional embedding.

The sequence  $\{\mathbf{z}_i^{(0)}\}_{i=1}^{N_p}$  is processed through  $L$  transformer layers. Each layer consists of Multi-Head Self-Attention (MSA) and Feed-Forward Network (FFN) blocks with residual connections:

$$\mathbf{z}^{(\ell)'} = \text{MSA} \left( \text{LN} \left( \mathbf{z}^{(\ell-1)} \right) \right) + \mathbf{z}^{(\ell-1)}, \quad (2)$$

$$\mathbf{z}^{(\ell)} = \text{FFN} \left( \text{LN} \left( \mathbf{z}^{(\ell)'} \right) \right) + \mathbf{z}^{(\ell)'}, \quad (3)$$

where LN is the layer normalization. The output  $\mathbf{z}^{(L)} \in \mathbb{R}^{N_p \times D}$  is hence reshaped to a feature map  $\mathbf{F} \in \mathbb{R}^{H/P \times W/P \times D}$ .

The feature map  $\mathbf{F}$  is upsampled using the segmentation decoder  $g_\psi : \mathbb{R}^{H/P \times W/P \times D} \rightarrow [0, 1]^{H \times W}$  to yield the soft prediction mask:

$$\hat{\mathbf{Y}} = g_\psi(\mathbf{F}), \quad (4)$$

where  $\psi$  denotes the parameters of the decoder, which consists of convolutional and upsampling layers. The overview of the proposed layer enhancement is provided in Fig.1.

### B. Loss Function

The total objective compound function is defined as a weighted sum of the pixel-wise cross-entropy loss  $\mathcal{L}_{\text{CE}}$  and the boundary-aware loss  $\mathcal{L}_{\text{B}}$ :

$$\mathcal{L}_{\text{total}} = \mathcal{L}_{\text{CE}}(\hat{\mathbf{Y}}, \mathbf{Y}) + \lambda \cdot \mathcal{L}_{\text{B}}(\hat{\mathbf{Y}}, \mathbf{Y}), \quad (5)$$

where  $\lambda \in \mathbb{R}_+$  balances the contributions of the two terms. Following [28], the boundary loss is defined using the ground truth signed distance map  $\phi_{\mathbf{Y}} : \Omega \rightarrow \mathbb{R}$  with a spatial domain  $\Omega$ :

$$\mathcal{L}_{\text{B}} = \frac{1}{|\Omega|} \sum_{x \in \Omega} \left| \phi_{\mathbf{Y}}(x) \cdot \hat{\mathbf{Y}}(x) \right|. \quad (6)$$

This encourages high prediction confidence near true boundaries and penalizes false positives/negatives in thin structures.



Fig. 1. Schematic of the transformer layers used in this work.

### C. Optimization Procedure

The model parameters  $\theta = \{\mathbf{E}, \mathbf{p}_i, \mathbf{w}, \psi\}$  are optimized via the Adam optimizer with weight decay and cosine learning rate schedule. Data augmentation  $\mathcal{A}$  is applied during training to enhance robustness:

$$\theta^* = \arg \min_{\theta} \mathbb{E}_{(\mathbf{X}, \mathbf{Y}) \sim \mathcal{D}} [\mathcal{L}_{\text{total}}(f_{\theta}(\mathcal{A}(\mathbf{X})), \mathbf{Y})]. \quad (7)$$

The provided pseudocode in the Algorithm 1 illustrates the training pipeline.

---

#### Algorithm 1 Boundary-Aware Vision Transformer

---

**Require:** Dataset  $\mathcal{D} = \{(\mathbf{X}_i, \mathbf{Y}_i)\}_{i=1}^N$ , loss weights  $\lambda$ , patch size  $P$ , number of layers  $L$

```

1: Initialize ViT parameters  $\theta$ 
2: for epoch = 1 to  $T$  do
3:   for each mini-batch  $\{(\mathbf{X}, \mathbf{Y})\}$  do
4:      $\mathbf{X} \leftarrow \mathcal{A}(\mathbf{X})$  // apply augmentations
5:     Divide  $\mathbf{X}$  into patches of size  $P \times P$ 
6:     Project patches to tokens and add positional embeddings
7:     Pass tokens through  $L$  Transformer layers
8:     Reshape and upsample output via segmentation head
9:     Compute  $\mathcal{L}_{\text{CE}}(\hat{\mathbf{Y}}, \mathbf{Y})$ 
10:    Compute signed distance map  $\phi_{\mathbf{Y}}$ 
11:    Compute boundary loss  $\mathcal{L}_{\text{B}}$ 
12:     $\mathcal{L}_{\text{total}} \leftarrow \mathcal{L}_{\text{CE}} + \lambda \cdot \mathcal{L}_{\text{B}}$ 
13:    Update  $\theta$  via backpropagation
14:   end for
15: end for
16: return Trained model  $f_{\theta}$ 

```

---

## IV. RESULTS AND DISCUSSION

### A. Implementation Details

The DCA-1 dataset consists of 134 angiographic images with expert-annotated ground truth labels provided by a board-certified cardiologist. To facilitate model development and evaluation, we adopted a standardized split protocol, allocating 104 images and the remaining 30 images, 77.6% and 22.4% for training and testing, respectively. Our Boundary-Aware Vision Transformer (BAVT) model is implemented using the PyTorch deep learning framework and trained on a single NVIDIA A100 GPU with 80 GB of VRAM. The model uses a plain ViT backbone with 12 transformer layers, 12 attention heads, and an embedding dimension of 768, totaling approximately 86 million parameters.

We use the Adam optimizer with a learning rate of  $1.5 \times 10^{-4}$  and weight decay of  $5 \times 10^{-3}$ . The learning rate

is scheduled using cosine annealing. Training is conducted with a batch size of 32, leveraging mixed precision (AMP) to reduce memory consumption.

Each input image is resized to  $512 \times 512$  and divided into non-overlapping patches of size  $16 \times 16$ . The transformer receives a sequence of 1024 tokens, each of dimension 768. A shallow segmentation decoder upsamples the output back to full resolution. The total training duration is set to 100 epochs.

a) *Data Preprocessing and Augmentation.*: Images are converted to grayscale and normalized using dataset-specific mean and standard deviation. We utilized the Adam optimizer with an initial learning rate of  $1e-4$ . To increase robustness and generalization, the following data augmentation strategies are applied:

- Random horizontal and vertical flipping with a probability of 0.5
- Random rotation in the range of  $[-15^\circ, +15^\circ]$
- Contrast Limited Adaptive Histogram Equalization (CLAHE)
- Gamma correction with values sampled from  $[0.8, 1.2]$
- Random elastic deformation with a probability of 0.3

All images from the DCA-1 dataset were used in their original grayscale format without resizing or cropping, allowing the network to process the full spatial context of vessel structures. The lack of a standardized training/testing split in the DCA-1 dataset necessitated manual partitioning; therefore, we performed experiments using four independent random splits to validate robustness. Model checkpoints were saved based on the lowest validation loss, and final evaluation was performed using the test split for each configuration.

### B. Performance Evaluation

We compared our method against state-of-the-art baselines including U-Net [20], Attention U-Net [29], U-Net++ [30], and RV-GAN [31], all trained under the same augmentation and grayscale input conditions. Quantitative comparisons are presented in Table I.

The performance of our Vision Transformer-based segmentation model was evaluated on the DCA-1 dataset, which consists of grayscale X-ray coronary angiograms. Due to the dataset's lack of an official benchmark split, we trained and evaluated the model across multiple randomized partitions. This protocol ensures fair and reproducible comparisons.

Our method demonstrated superior segmentation quality across sensitivity, specificity, IoU, and AUC metrics, surpassing conventional CNN-based models. In contrast to convolutional architectures that often struggle with fine vessel boundaries, our ViT-based model leverages global self-attention to

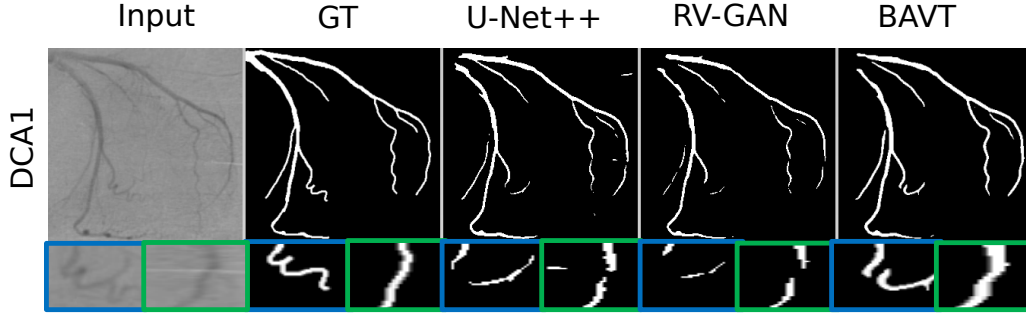


Fig. 2. Qualitative comparison of segmentation results on the DCA-1 dataset: ground truth (GT) and predictions from U-Net++, RV-GAN, and the proposed BAVT model. BAVT demonstrates more continuous and anatomically accurate vessel structures, particularly in thin branches.

TABLE I  
PERFORMANCE COMPARISON ON THE DCA-1 DATASET

Methods	Sen.	Spe.	F1	Acc.	AUC	IoU
U-Net	0.7812	0.9721	0.7951	0.9653	0.9734	0.6542
Att. U-Net	0.7623	0.9847	0.7798	0.9691	0.9825	0.6389
U-Net++	0.7272	0.9815	0.7520	0.9632	0.9702	0.6113
RV-GAN	0.7110	<b>0.9905</b>	0.7701	0.9724	0.9878	0.6331
<b>BAVT</b>	<b>0.8365</b>	0.9844	<b>0.7909</b>	<b>0.9757</b>	<b>0.9918</b>	<b>0.6559</b>

**Note:** Sen. stands for Sensitivity, Spe. for Specificity, F1 for F1-score, Acc. for Accuracy, AUC for Area Under Curve, IoU for Intersection over Union, respectively. The proposed method is indicated as BAVT.

TABLE II  
ABLATION STUDY ON THE EFFECT OF EDGE-AWARE BLOCK IN ViT ARCHITECTURE ON DCA-1 DATASET

Methods	Sen.	Spe.	F1	Acc.	AUC	IoU
ViT (Baseline)	0.7935	0.9822	0.7675	0.9728	0.9874	0.6356
<b>BAVT (Ours)</b>	<b>0.8365</b>	<b>0.9844</b>	<b>0.7909</b>	<b>0.9757</b>	<b>0.9918</b>	<b>0.6559</b>

**Note:** Sen. - Sensitivity, Spe. - Specificity, F1 - F1-score, Acc. - Accuracy, AUC - Area Under Curve, IoU - Intersection over Union.

preserve thin and elongated vessel connectivity. Notably, it achieved higher sensitivity, reflecting its capability to recover microvasculature structures more effectively.

Comparisons of segmentation results with U-Net++, RV-GAN, and proposed BAVT model on representative samples from the DCA-1 dataset are presented in Figure 2. While U-Net++ and RV-GAN exhibit satisfactory performance on major vessels, both models tend to either over-smooth boundaries or fragment thin branches—resulting in incomplete or disconnected vascular structures.

In contrast, BAVT demonstrates superior boundary adherence and microvessel continuity. The edge-aware supervision incorporated during training enables the model to recover challenging structures that are often missed by CNN-based or GAN models.

### C. Ablation Study. Edge-Awareness in ViT

To quantify the contribution of edge-awareness, we performed an ablation study comparing the full proposed BAVT with a classical ViT baseline. The baseline uses the same transformer backbone and decoder structure but omits the boundary loss module during training.

As shown in Table II, removing the edge-awareness significantly impacts the model’s sensitivity and IoU. Specifically, the classical ViT yields a sensitivity of 0.7942, compared to 0.8365 in BAVT. This suggests that the edge-aware formulation helps recover finer vessel structures, particularly at thin branches and junctions, where ViT alone tends to under-segment due to smoothing effects of global attention.

Furthermore, the boundary-aware loss contributes to an improvement in F1 score from 0.7691 to 0.7909, and AUC from 0.9874 to 0.9918, demonstrating that guiding the transformer decoder with geometric priors improves both pixel-wise and structural accuracy.

The ablation confirms the critical role of boundary-aware supervision in enhancing segmentation performance on angiographic datasets characterized by sparse, elongated features.

### D. Model Efficiency

Although transformer-based models typically involve higher computational costs compared to classical CNNs, the proposed BAVT remains computationally feasible on modern hardware such as NVIDIA A100 and H100 GPUs. The total complexity of BAVT is estimated at approximately 130–140 GFLOPs per forward pass for a  $512 \times 512$  input, primarily due to the self-attention operations over 1024 tokens in the ViT backbone.

While our model is not optimized for extreme lightweight deployment, its architectural simplicity and full compatibility with vision foundation model pretraining make it both scalable and effective. The added boundary-aware supervision introduces only marginal overhead, yet yields substantial gains in segmentation accuracy—particularly for fine-grained vascular structures that are often missed by more lightweight or convolution-only models. These trade-offs make BAVT a practical and performant solution for clinical-grade vessel segmentation tasks.

## V. CONCLUSIONS

In this work, we proposed Boundary-Aware Vision Transformer, BAVT, for the task of vascular segmentation in coronary angiography. Our method addresses a key limitation of classical ViT models by integrating a boundary-aware loss that enhances the model's ability to delineate fine vessel structures, including microvascular branches. Unlike prior approaches that rely on hybrid CNN-transformer architectures or complex decoders, BAVT maintains a ViT-based design, which makes it compatible with modern vision foundation models pretraining strategies.

Results demonstrated the effectiveness of BAVT on the DCA-1 dataset, where it outperforms both CNN baselines and transformer hybrids across all major metrics. The conducted ablation study confirms the significant performance gains introduced by the edge-aware supervision, specifically in terms of IoU crucial for vessel network assessments.

Future work will explore extensions of this architecture to 3D angiographic sequences and multi-view vessel tracking. Additionally, we aim to investigate integrating uncertainty estimation into the ViT pipeline to improve clinical trustworthiness and usability.

## ACKNOWLEDGMENT

Part of this work was supported by the Skolkovo Institute of Science and Technology - University of Sharjah Joint Projects: Artificial Intelligence for Life, project "Towards an Explainable Diabetic Retinopathy Grading Model".

## REFERENCES

- [1] B. Jing, P. Xie, and E. Xing, "On the automatic generation of medical imaging reports," *arXiv preprint arXiv:1711.08195*, 2017.
- [2] Y. Li, X. Liang, Z. Hu, and E. P. Xing, "Hybrid retrieval-generation reinforced agent for medical image report generation," *Advances in neural information processing systems*, vol. 31, 2018.
- [3] L. Delrue, R. Gosselin, B. Ilsen, A. Van Landeghem, J. de Mey, and P. Duyck, "Difficulties in the interpretation of chest radiography," *Comparative interpretation of CT and standard radiography of the chest*, pp. 27–49, 2011.
- [4] A. Selivanov, O. Y. Rogov, D. Chesakov, A. Shelmanov, I. Fedulova, and D. V. Dylov, "Medical image captioning via generative pretrained transformers," *Scientific Reports*, vol. 13, Mar. 2023.
- [5] Y. Jiang and Y. Shen, "M4oE: A Foundation Model for Medical Multimodal Image Segmentation with Mixture of Experts," in *proceedings of Medical Image Computing and Computer Assisted Intervention – MICCAI 2024*, vol. LNCS 15012, Springer Nature Switzerland, October 2024.
- [6] Y. Cao, L. Cui, L. Zhang, F. Yu, Z. Li, and Y. Xu, "Mmtm: multi-modal memory transformer network for image-report consistent medical report generation," in *Proceedings of the AAAI Conference on Artificial Intelligence*, vol. 37, pp. 277–285, 2023.
- [7] J. Wang, Z. Yang, X. Hu, L. Li, K. Lin, Z. Gan, Z. Liu, C. Liu, and L. Wang, "Git: A generative image-to-text transformer for vision and language," *arXiv preprint arXiv:2205.14100*, 2022.
- [8] T. Tanida, P. Müller, G. Kaissis, and D. Rueckert, "Interactive and explainable region-guided radiology report generation," in *Proceedings of the IEEE/CVF Conference on Computer Vision and Pattern Recognition*, pp. 7433–7442, 2023.
- [9] S. Bu, T. Li, Y. Yang, and Z. Dai, "Instance-level expert knowledge and aggregate discriminative attention for radiology report generation," in *Proceedings of the IEEE/CVF Conference on Computer Vision and Pattern Recognition*, pp. 14194–14204, 2024.
- [10] G. Zhao, Z. Zhao, W. Gong, and F. Li, "Radiology report generation with medical knowledge and multilevel image-report alignment: A new method and its verification," *Artificial Intelligence in Medicine*, vol. 146, p. 102714, 2023.
- [11] A. Vaswani, N. Shazeer, N. Parmar, J. Uszkoreit, L. Jones, A. N. Gomez, L. u. Kaiser, and I. Polosukhin, "Attention is All you Need," in *NeurIPS*, 2017.
- [12] A. Dosovitskiy, L. Beyer, A. Kolesnikov, D. Weissenborn, X. Zhai, T. Unterthiner, M. Dehghani, M. Minderer, G. Heigold, S. Gelly, J. Uszkoreit, and N. Houlsby, "An Image is Worth 16x16 Words: Transformers for Image Recognition at Scale," in *ICLR*, 2021.
- [13] Z. Liu *et al.*, "Swin transformer: Hierarchical vision transformer using shifted windows," in *Proceedings of the IEEE/CVF international conference on computer vision*, pp. 10012–10022, 2021.
- [14] E. Xie, W. Wang, Z. Yu, A. Anandkumar, J. M. Alvarez, and P. Luo, "SegFormer: Simple and Efficient Design for Semantic Segmentation with Transformers," in *NeurIPS*, 2021.
- [15] Z. Chen, Y. Duan, W. Wang, J. He, T. Lu, J. Dai, and Y. Qiao, "Vision Transformer Adapter for Dense Predictions," in *ICLR*, 2023.
- [16] M. Oquab, T. Darcet, T. Moutakanni, H. Vo, M. Szafraniec, V. Khalidov, P. Fernandez, D. Haziza, F. Massa, A. El-Nouby, *et al.*, "DINOv2: Learning Robust Visual Features without Supervision," *TMLR*, 2024.
- [17] Y. Fang, Q. Sun, X. Wang, T. Huang, X. Wang, and Y. Cao, "EVA-02: A Visual Representation for Neon Genesis," *Image and Vision Computing*, 2024.
- [18] W. Chen, X. Du, F. Yang, L. Beyer, X. Zhai, T.-Y. Lin, H. Chen, J. Li, X. Song, Z. Wang, *et al.*, "A Simple Single-Scale Vision Transformer for Object Localization and Instance Segmentation," in *ECCV*, 2022.
- [19] Y. Fang, B. Liao, X. Wang, J. Fang, J. Qi, R. Wu, J. Niu, and W. Liu, "You Only Look at One Sequence: Rethinking Transformer in Vision through Object Detection," in *NeurIPS*, 2021.
- [20] O. Ronneberger, P. Fischer, and T. Brox, "U-net: Convolutional networks for biomedical image segmentation," in *International Conference on Medical image computing and computer-assisted intervention*, pp. 234–241, Springer, 2015.
- [21] X. Hu, L. Wang, and Y. Li, "Ht-net: A hybrid transformer network for fundus vessel segmentation," *Sensors*, vol. 22, no. 18, p. 6782, 2022.
- [22] Y. Jiang *et al.*, "Mtpa\_unet: Multi-scale transformer-position attention retinal vessel segmentation network joint transformer and cnn," *Sensors*, vol. 22, no. 12, p. 4592, 2022.
- [23] J. Deng, W. Dong, R. Socher, L.-J. Li, K. Li, and L. Fei-Fei, "ImageNet: A large-scale hierarchical image database," in *CVPR*, 2009.
- [24] M. Caron, H. Touvron, I. Misra, H. Jégou, J. Mairal, P. Bojanowski, and A. Joulin, "Emerging Properties in Self-Supervised Vision Transformers," in *ICCV*, 2021.
- [25] T. Kerssis, D. De Geus, and G. Dubbelman, "How to Benchmark Vision Foundation Models for Semantic Segmentation?," in *CVPR Workshops*, 2024.
- [26] M. N. Getahun, O. Y. Rogov, D. V. Dylov, A. Somov, A. Bouridane, and R. Hamoudi, "Fs-net: Full scale network and adaptive threshold for improving extraction of micro-retinal vessel structures," *Pattern Recognition Letters*, vol. 189, pp. 188–194, 2025.
- [27] Z. Liu, H. Mao, C.-Y. Wu, C. Feichtenhofer, T. Darrell, and S. Xie, "A ConvNet for the 2020s," in *CVPR*, 2022.
- [28] H. Kervadec, J. Bouchtiba, C. Desrosiers, E. Granger, J. Dolz, and I. Ben Ayed, "Boundary loss for highly unbalanced segmentation," in *Proceedings of The 2nd International Conference on Medical Imaging with Deep Learning (M. J. Cardoso, A. Feragen, B. Glocker, E. Konukoglu, I. Oguz, G. Unal, and T. Vercauteren, eds.)*, vol. 102 of *Proceedings of Machine Learning Research*, pp. 285–296, PMLR, 08–10 Jul 2019.
- [29] O. Oktay *et al.*, "Attention u-net: Learning where to look for the pancreas," *arXiv preprint arXiv:1804.03999*, 2018.
- [30] Z. Zhou, M. M. Rahman Siddiquee, N. Tajbakhsh, and J. Liang, "Unet++: A nested u-net architecture for medical image segmentation," in *Deep Learning in Medical Image Analysis and Multimodal Learning for Clinical Decision Support: 4th International Workshop, DLMIA 2018, and 8th International Workshop, ML-CDS 2018, Held in Conjunction with MICCAI 2018, Granada, Spain, September 20, 2018, Proceedings 4*, pp. 3–11, Springer, 2018.
- [31] S. A. Kamran *et al.*, "Rv-gan: segmenting retinal vascular structure in fundus photographs using a novel multi-scale generative adversarial network," in *International Conference on Medical Image Computing and Computer-Assisted Intervention*, pp. 34–44, Springer, 2021.